ACTIVE MEDIA DOI: 10.1070/QEL16029

Experimental results on the dissociation of molecular iodine in the presence of singlet oxygen molecules

M.V. Zagidullin, N.A. Khvatov, M.S. Malyshev, M.I. Svistun

Abstract. **The experimental results on the dissociation of iodine molecules in the presence of single oxygen molecules under a wide-range variation of the oxygen–iodine composition are presented. The rate constants are determined as 4.3×10^{-17} cm^3 s^{-1} for the reaction $O_2(^1\Delta) + O_2(^1\Delta) \rightarrow O_2(^1\Sigma) + O_2(^3\Sigma)$ (reaction 1), 2.8×10^{-13} cm^3 s^{-1} for the reaction $O_2(^1\Delta) + I(^2P_{1/2}) \rightarrow O_2(^1\Sigma) + I(^2P_{3/2})$ (4) and 8.3×10^{-11} cm^3 s^{-1} for the reaction $O_2(^1\Sigma) + I_2 \rightarrow O_2(^3\Sigma) + 2I$ (2). The analysis of the experimental results shows that for different compositions of the active medium of the oxygen–iodine laser the iodine dissociation occurs via the chain of reactions 1, 2, $O_2(^1\Delta) + I(^2P_{3/2}) \rightarrow O_2(^3\Sigma) + I(^2P_{1/2})$, 4 and in the cascade process $I_2 + I(^2P_{1/2}) \rightarrow I_2(v) + I(^2P_{3/2})$, $I_2(v) + O_2(^1\Delta) \rightarrow 2I + O_2(^3\Sigma)$. For typical active medium compositions of the supersonic chemical oxygen–iodine laser, the contributions of each of the mechanisms to the dissociation are comparable. The experiments carried out did not reveal any contribution from the vibrationally excited oxygen molecules to the iodine dissociation. Thus, the performed experiments and the conclusions drawn from them completely confirm the mechanism of iodine dissociation, proposed earlier.**

Keywords: *singlet oxygen, iodine dissociation, oxygen–iodine laser.*

1. Introduction

The molecular iodine dissociation plays the key role in the formation of the active medium of the chemical oxygen–iodine laser (COIL). For the first time the iodine molecule dissociation in the presence of singlet oxygen molecules was observed in Ref. [1]. For the iodine dissociation process a few mechanisms were proposed, the main reactions that occur in the COIL active medium being presented in Table 1. According to the first of them [1, 2], the dissociation occurs as a result of sequential reactions 1–4. However, it appeared impossible to provide the experimentally observed rate of the iodine dissociation at the expense of reactions 1–4, and, therefore, the additional dissociation mechanism was proposed, including reactions 6–8 [3]. In reactions 6, 7, the iodine molecule can be produced in the maximally excited vibrational state $v = 40$. In reactions 8, the total energy of interacting particles is sufficient for the iodine dissociation, if they occupy the vibrational level not lower than $v = 20$. The dissociation in the stepwise mechanism including reactions 10, 11 is possible [1, 4, 5]. The vibrationally excited oxygen molecules can appear as a result of reactions 1, 4 [6, 7] and in the course of deactivation of the molecules $O_2(a)$, $O_2(b)$. As a result of fast resonance V–V and E–E exchanges, the vibrationally excited $O_2(a)$ molecules are produced [8–10]. The iodine dissociation can occur in reactions 14 [2, 11] or 15, since the total energy of $O_2(a^1\Delta)$ and $I(^2P_{1/2})$ exceeds the dissociation energy of the iodine molecule. To calculate the gain and the output power of the COIL, the proposed mechanisms were used both separately and in combination [12–15].

The rate of molecular iodine dissociation in the presence of singlet oxygen also plays the key role in the practical implementation of an optically pumped oxygen–iodine laser [16]. In the present paper, we present the experimental results on the iodine dissociation in the environment of singlet oxygen within a wide range of the oxygen–iodine medium composi-

Table 1. Reactions in the oxygen–iodine medium.

Reaction number	Reaction
1	$O_2(a) + O_2(a) \rightarrow O_2(b) + O_2(X)$
2	$O_2(b) + I_2 \rightarrow O_2(X) + 2I$
3	$O_2(a) + I \rightarrow O_2(X) + I^*$
4	$O_2(a) + I^* \rightarrow O_2(b) + I$
5	$O_2(b) + M \rightarrow O_2(X)\ (O_2(a)) + M$
6	$I_2 + O_2(a) \rightarrow I_2(20 \leqslant v \leqslant 40) + O_2(X)$
7	$I_2 + I^* \rightarrow I_2 + I$
8a	$I_2(v) + O_2(a) \rightarrow 2I + O_2(X)$
8b	$I_2(v) + I^* \rightarrow 2I + I$
9	$I_2(20 \leqslant v \leqslant 40) + M \rightarrow I_2(v < 20) + M$
10a	$O_2(a, v = 1) + I_2(X) \rightarrow O_2(X, v = 0) + I_2(A)$
10b	$O_2(a, v = 2) + I_2(X) \rightarrow O_2(X, v = 0) + I_2(A)$
11a	$I_2(A) + O_2(a) \rightarrow 2I + O_2(X)$
11b	$I_2(A) + I^* \rightarrow 2I + I$
12	$I_2(A) + M \rightarrow I_2(X) + M$
13	$O_2(v) + M \rightarrow O_2(v - 1) + M$
14	$O_2(a) + O_2(a) + I_2 \rightarrow 2I + 2O_2(X)$
15	$O_2(a) + I^* + I_2 \rightarrow 3I + O_2(X)$

Note: $O_2(X)$, $O_2(a)$, $O_2(b)$ are the oxygen molecules in the states $^3\Sigma$, $^1\Delta$, $^1\Sigma$; I, I* – are the iodine atoms in the states $^2P_{3/2}$, $^2P_{1/2}$; $I_2(20 \leqslant v \leqslant 40)$ is the iodine molecule in the vibrational state with $20 \leqslant v \leqslant 40$; $I_2(A)$ is the iodine molecule in the state $A^3\Pi_{2u}$ or $A^3\Pi_{1u}$; and $O_2(v)$ is the oxygen molecule in the vibrationally excited state.

M.V. Zagidullin Samara Branch, P.N. Lebedev Physics Institute, Russian Academy of Sciences, ul. Novosadovaya 221, 443086 Samara, Russia; Samara National Research University, Moskovskoe sh. 34, 443086 Samara, Russia; e-mail: marsel@fian.smr.ru;
N.A. Khvatov, M.I. Svistun Samara Branch, P.N. Lebedev Physics Institute, Russian Academy of Sciences, ul. Novosadovaya 221, 443086 Samara, Russia;
M.S. Malyshev Samara National Research University, Moskovskoe sh. 34, 443086 Samara, Russia

Received 5 February 2016; revision received 27 April 2016
Kvantovaya Elektronika **46** (8) 706–712 (2016)
Translated by V.L. Derbov

tions. The aim of the experiments was to reveal the mechanism or a few mechanisms, most precisely describing the observed features of the iodine dissociation.

2. Experiment

The schematic of the experimental setup is presented in Fig. 1. A singlet oxygen generator (SOG) in gas phase produced an oxygen flow up to 1 millimole per second with the content of singlet oxygen $O_2(a^1\Delta)$ above 50%, which passed through a water vapour trap (WVT), consisting of an array of parallel gas-flow channels, submerged in a bath with cooled ethanol. Downstream, two mixing units were placed sequentially with the purpose to supply additional gases (water vapours, carbon dioxide, argon, oxygen) to the main flow. After the second mixing unit, the emission corresponding to the a → X transition in the O_2 molecules was detected in the flow using a germanium photodetector, equipped with a broadband filter, and the b → X emission of the O_2 molecules (λ = 762 nm) was detected using a monochromator. The constant time-independent intensity of these radiations indicated the constant concentration of O_2(a) and O_2(b) at the entrance to the optical diagnostic section (ODS) during the experiment. Through a system of cylindrical channels the main flow arrived at the ODS, implemented as a silica tube with an inner diameter 15 mm and a length L_{ODS} = 350 mm. The mixture of molecular iodine and argon was admixed to the main flow via an injector in the form of an array of nine parallel tubes (the length 25 mm, the inner diameter 2 mm, the wall thickness 0.1 mm). According to our estimates, in this construction the effective length of laminar mixing of flows should amount to less than 1 mm for the operating gas velocities in the ODS up to 30 m s^{-1} and the pressure smaller than 5 Torr. The gas flew out from the ODS through the delivery outlet, in which the flow velocity was equal to the velocity of sound.

The dosing of gases and the measurement of their consumption from the commercial gas vessels (Ar, CO_2, O_2) was performed using a Mass–View electronic gas flowmeter (Bronkhorst). The molar consumption of the oxygen, supplied to the ODS from the SOG, does not coincide with the consumption of chlorine, supplied to the SOG, since part of the gas leaves it with the worked-out liquid. The consumption of the oxygen coming to the ODS from the SOG was determined in the following way. The pressure in the ODS was measured, and when the experiment was finished, the oxygen was supplied to it from a commercial vessel. By varying this supply, the pressure in the ODS was restored to the value measured in the course of the experiment. The consumption of the oxygen from the vessel was assumed to equal that in the SOG during the experiment. At the input and output of the ODS, the pressure was measured, the mean value of which was used to calculate the mean gas velocity in the ODS.

The receiving face of a double-channel optical fibre cable, contacting with the ODS wall, could move along it on a carriage driven by a linear translator. One of the output cable channels was connected with the input slit of an M266 spectrometer, which recorded the radiation, corresponding to the transition a → X (λ = 1268 nm) of the oxygen molecule and the transition $^2P_{1/2} \rightarrow {}^2P_{3/2}$ (1315 nm) of the iodine atom. The second channel was connected with the input of an Avantes-2048 spectrometer, which recorded the radiation, corresponding to the transition b → X (λ = 762 nm) of the oxygen molecule. The absolute energy calibration of the fibre–spectrometer–detector system was carried out using an AvaLight-Hal-Cal etalon light source (Avantes). The absolute calibration error was determined mainly by the potential accuracy of the etalon source spectral luminosity equal to 9.5%. The flow temperature in the ODS was determined from the partially resolved rotational spectral structure of the transition b → X of the oxygen molecule [17]. In all experiments the temperature of the gas in the ODS amounted to 300±10 K. From the results of the measurements we determined the concentrations of the electronically excited molecules O_2(a), O_2(b), and the atoms $I(^2P_{1/2})$, the total concentration of iodine atoms, and the relative fraction of singlet oxygen [18, 19].

3. Experimental results

The rate constants k_1, k_2, k_4 have been measured by us earlier [18–20]. (Hereafter, k_i denotes the rate constant of the ith reaction in Table 1.) Keeping in mind the important role of these reactions in the dissociation mechanism, we have measured their rate constants again using the setup described above. Generally, the new measurements confirmed the values of the rate constants of reactions 1 and 4, obtained by us earlier. The following equalities take place

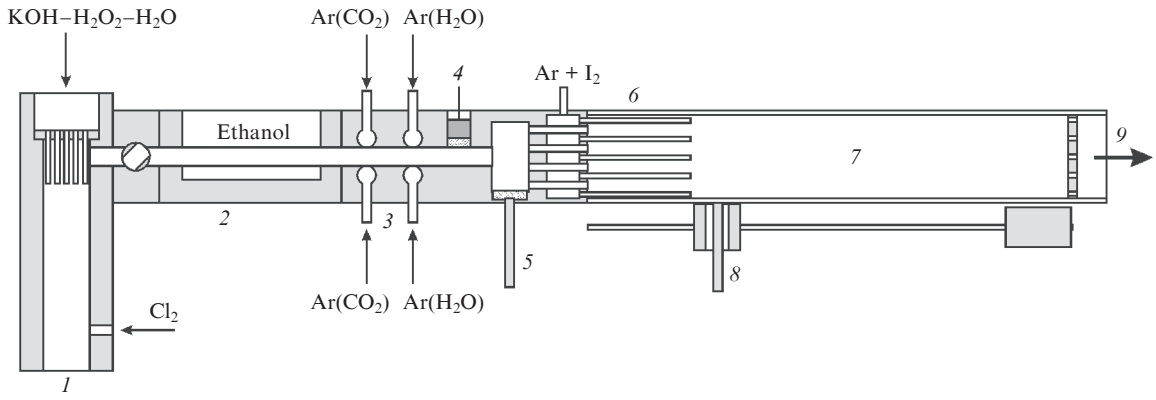

Figure 1. Schematic of the experiment using a gas-flow optical diagnostic section:
(*1*) SOG; (*2*) WVT; (*3*) mixing units; (*4*) germanium detector; (*5*) receiving end of the fibre for the radiation coupling into the monochromator; (*6*) molecular iodine injector; (*7*) ODS; (*8*) moveable carriage with the receiving end of the fibre to launch radiation into the monochromator; (*9*) consumption washer.

$$\frac{k_1}{k_5(CO_2)} = (1.04 \pm 0.04)\times 10^{-4}, \quad \frac{k_4}{k_5(CO_2)} = 0.69 \pm 0.04,$$

where $k_5(CO_2)$ is the rate constant of reaction 5 for M = CO_2. From these equalities it follows that $K = k_4/k_1 \approx 6600$. This value is comparable with K = 5500 from Ref. [21]. The measured values of $k_5(CO_2)$ are scattered within the range 3.0×10^{-13} cm^3 s^{-1} [22]–6.1×10^{-13} cm^3 s^{-1} [23]. Using the recommended value $k_5(CO_2) = 4.1\times10^{-13}$ cm^3 s^{-1} from the database on atmospheric chemistry IUPAC ([24], http://iupac.pole-ether.fr), we obtain $k_1 = (4.3\times0.2)\times10^{-17}$ cm^3 s^{-1} and $k_4 = (2.8\pm0.2)\times10^{-13}$ cm^3 s^{-1}. These values are close to those obtained in Refs [18–20], but are greater than those reported in Refs [25–27] by nearly two times.

Let us consider in detail the measurements of the rate constant for reaction 2. The quasi-stationary concentration of the molecules O_2(b) is determined by reactions 1, 2, 4 and 5:

$$n_b = \frac{k_1 n_a^2}{\Gamma_b + k_2 n_{I_2}}\left(1 + K\frac{n_{I*}}{n_a}\right), \qquad (1)$$

where n_a, n_b, n_{I_2} are the concentrations of the molecules O_2(a), O_2(b), I_2; n_{I*} is the concentration of the excited iodine atoms $I(^2P_{1/2})$; $\Gamma_b = \Gamma_0 + \sum_M k_5(M)n_M$ is the deactivation rate of the molecules O_2(b); and Γ_0 is the rate of their deactivation at the walls. Approximation (1) will be valid if the time Γ_b^{-1} is much smaller than the time of deactivation of O_2(a) and the time of iodine dissociation. The quasi-stationary concentrations of the molecules $I_2(^1\Sigma, 20 \leqslant v \leqslant 40)$ and I_2(A) are

$$\begin{aligned} n_{I_2}(v) &= n_{I_2}(k_6 n_a + \varphi k_7 n_{I*})Q_{I_2}^{-1}, \\ n_A &= n_{I_2}(k_{10a}f_1 + k_{10b}f_2)n_a Q_A^{-1}, \end{aligned} \qquad (2)$$

where $Q_{I_2}^{-1} = k_{8a}n_a + k_{8b}n_{I*} + \Gamma_{I_2v}$; $Q_A^{-1} = k_{11a}n_a + k_{11b}n_{I*} + \Gamma_{I_2A}$; $n_{I_2}(v)$ is the concentration of vibrationally excited molecules I_2 ($20 \leqslant v \leqslant 40$); n_A is the concentration of the I_2(A) molecules; φ is the probability of formation of vibrationally excited iodine molecules in reaction 7 with v within the range 20–40; f_1 and f_2 are the relative content of vibrationally excited molecules of singlet oxygen O_2(a, v = 1) and O_2(a, v = 2), respectively; $\Gamma_{I_2v} = \sum_M k_9(M)n_M$ is the rate of relaxation of vibrationally excited ($20 \leqslant v \leqslant 40$) I_2 molecules; $\Gamma_{I_2A} = \sum_M k_{12}(M)$ n_M is the rate of deactivation of the I_2(A) molecules; and n_M is the concentration of particles M.

With Eqns (1) and (2) taken into account, the dissociation of iodine in the ODS is described by the equation

$$\begin{aligned} V\frac{dn_{I_2}}{n_{I_2}dz} &= -k_2 n_b - (\hat{k}_{6a} + \hat{k}_{6b} + \hat{k}_{11a} + \hat{k}_{11b})n_a \\ &\quad - (\hat{k}_{7a} + \hat{k}_{7b})n_{I*} - (k_{14}n_a^2 + k_{15}n_a n_{I*}), \end{aligned} \qquad (3)$$

where z is the distance from the beginning of the ODS along its axis; V is the gas velocity; $\hat{k}_{6a} = k_6 k_{8a} n_a Q_{I_2}^{-1}$; $\hat{k}_{6b} = k_6 k_{8b} n_{I*} Q_{I_2}^{-1}$; $\hat{k}_{7a} = \varphi k_7 k_{8a} n_a Q_{I_2}^{-1}$; $\hat{k}_{7b} = \varphi k_7 k_{8b} n_{I*} Q_{I_2}^{-1}$; $\hat{k}_{11a} = k_{11a}n_a(k_{10a}f_1 + k_{10b}f_2)Q_A^{-1}$; and $\hat{k}_{11b} = k_{11b}n_{I*}(k_{10a}f_1 + k_{10b}f_2)Q_A^{-1}$.

Consider the stage of initiating the I_2 dissociation, i.e., the case of very small concentrations of iodine, when $\Gamma_b \gg k_2 n_{I_2}$, $n_{I*}/n_a \ll K^{-1}$, and reactions 7, 8b, 11b involving the excited iodine atoms play a insignificant role during the entire dissociation time. Then, putting $n_{I*} = 0$ in Eqns (1)–(3), we obtain

$$V\frac{dn_{I_2}}{n_{I_2}dz} = -K_d, \qquad (4)$$

where $K_d = k_2 n_b^0 + (\hat{k}_{6a} + \hat{k}_{11a} + k_{14}n_a)n_a$ is the dissociation rate; and $n_b^0 = k_1 n_a^2 \Gamma_b^{-1}$ is the concentration of the O_2(b) molecules at the input of the ODS. The solution of Eqn (4) at the constant value of K_d yields the variation of the total concentration n_I of iodine atoms along the ODS axis:

$$n_I = 2n_{I_2}^0[1 - \exp(-K_d z/V)]. \qquad (5)$$

In practice the constant value of K_d was achieved by reducing the iodine consumption (or the observed value of n_{I*}) until the profile of the concentration n_{I*} was independent of the iodine consumption, and the concentrations O_2(a) and O_2(b) became constant along the ODS [19]. In the present work it was valid for $n_{I*} < 10^{11}$ cm^{-3}. From the measured values of n_I, using Eqn (5) the values of K_d were determined, which are presented in Fig. 2 as dependences on the concentration of O_2(b) molecules. The quantity K_d is seen to depend neither on the concentration of O_2(a), nor on the gas type (CO_2 or H_2O) used to dose the concentration of O_2(b). The approximation of K_d in the form of a linear function $K_a + k_2 n_b$ yields $k_2 = (8.3\pm0.3)\times10^{-11}$ cm^3 s^{-1} and $K_a = 38.5$ s$^{-1} \pm \delta K_d$, where $\delta K_d = 5$ s^{-1}. This value of k_2 slightly differs from the value $(9.3\pm2)\times10^{-11}$ cm^3 s^{-1} obtained in Ref. [19] under different experimental conditions and is comparable with the values 5.9×10^{-11} cm^3 s^{-1} [28] and 7×10^{-11} cm^3 s^{-1} [29], obtained for the total rate constant of the reaction of O_2(b) deactivation by the iodine molecules. The nonzero value of K_a independent of n_a is explained by us as due to the systematic error, caused by the transverse inhomogeneities of the gas flow velocity and the concentrations of medium components because of the viscous laminar flow in the ODS [30].

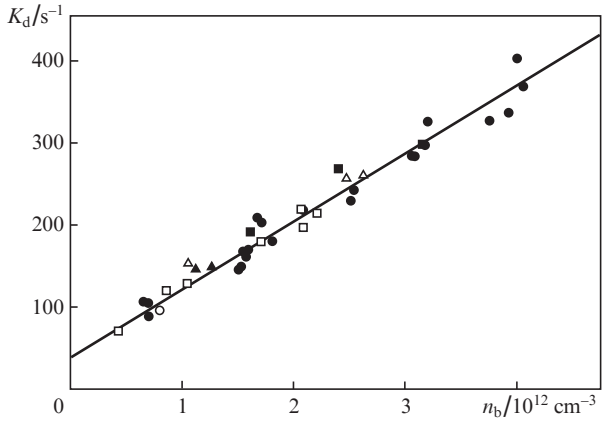

Figure 2. Dependences of K_d on the concentration of O_2(b) molecules at low initial concentrations of iodine molecules ($n_{I_2} < 10^{11}$ cm^{-3}) for the media O_2–Ar–H_2O (dark symbols) and O_2–Ar–CO_2 (light symbols). The concentration of O_2(a) molecules is 10^{16} cm^{-3} (circles), 2×10^{16} cm^{-3} (squares) and 3×10^{16} cm^{-3} (triangles).

Let us estimate the contribution of other processes to the iodine dissociation at the stage, when the concentration of $I(^2P_{1/2})$ atoms is still small. The variation of the O_2(a) concentration in the resent experiments by $\delta n_a = 2\times10^{16}$ cm^{-3} could lead to a change in K_a not exceeding $\delta K_d = 5$ s^{-1}. Therefore, $k_6 \leqslant \delta K_d/\delta n_a = 2.5\times10^{-16}$ cm^3 s^{-1}, which agrees with the estimate $k_6 < 5\times10^{-16}$ cm^3 s^{-1} from Ref. [28]. The iodine dissociation as a result of reactions 6, 8a potentially can compete with that due to reactions 1, 2 under the condition that $n_b/n_a < k_6/k_2 < 3\times10^{-6}$. For the mixture O_2–I_2–H_2O with a low

initial concentration of iodine, the relation $n_b^0 = k_1 n_a^2 \Gamma_b^{-1}$ is approximately valid, where $\Gamma_b = k_5(H_2O) n_{H_2O}$ and $k_5(H_2O) = 4.3\times10^{-12}$ cm^3 s^{-1} [24]. Then the contribution to the dissociation from reactions 6, 8a can be comparable with that of reactions 1, 2 at the relative water content $n_{H_2O}/n_a > (k_1/k_5(H_2O))(k_2/k_6) = 3$. For the mixture $O_2-I_2-H_2O$ with a very high initial concentration of iodine the relation $n_b = k_1 n_a^2/(k_2 n_{I_2})$ is approximately valid. In this case the contribution of reactions 6–8a can be comparable with that of reactions 1, 2, if $n_{I_2}/n_a \approx (k_1/k_6) > 0.17$. Usually for the active medium of an oxygen-iodine laser the conditions $n_{H_2O}/n_a < 1$ and $n_{I_2}/n_a < 0.05$ are valid, so that for the COIL active medium the contribution of reactions 6, 8a to the iodine dissociation, is negligibly small, even if it exists at all.

Let us estimate the role of the reaction k_{14} at the initiating stage of dissociation. When the O_2(a) concentration changes from 10^{16} to 3×10^{16} cm^{-3} the variation of the constant K_d does not exceed δK_d. From this fact we get the estimate $k_{14} < \delta K_d/(8\times10^{32}\ \text{cm}^{-6}) \approx 6\times10^{-33}$ cm^6 s^{-1}, which is essentially smaller than 6×10^{-29} cm^6 s^{-1} from Ref. [11]. The contribution of reaction 14 to the dissociation of I_2 can be comparable with that of reactions 1, 2 under the condition that $k_{14} n_a^2 \approx k_2 n_b$. For small iodine concentrations, when $n_b^0 = k_1 n_a^2 \Gamma_b^{-1}$, this equality is valid when $n_{H_2O} \approx k_1 k_2/(k_{14} k_5(H_2O)) > 10^{17}$ cm^{-3}. For a large iodine concentration, when $n_b = k_1 n_a^2/(k_2 n_{I_2})$, the contribution of reaction 14 can be comparable with that of reactions 1, 2 at the initiating stage (when $n_{I^*} \approx 0$), if $n_{I_2} > k_1/k_{14} > 7\times10^{15}$ cm^{-3}. Both mentioned cases do not take place in the active medium of the COIL, since usually the concentrations of water and iodine in it are essentially smaller than the above extreme values.

In Ref. [31], the relative content of vibrationally excited O_2 molecules at the output of the chemical SOG is shown to be close to the equilibrium value. At the gas temperature near 300 K the relative equilibrium contents of O_2(a, $v = 1$) and O_2(a, $v = 2$) are equal to $f_1 \approx 10^{-3}$ and $f_2 \approx 10^{-6}$. The change in the O_2(a) concentration from 10^{16} to 3×10^{16} cm^{-3} must lead to a triple increase in the concentration of vibrationally excited O_2(a) molecules. In our experiments the influence of the vibrationally excited O_2(a) molecules on the rate of initiating the iodine dissociation is within the values not exceeding $\delta K_d = 5$ s^{-1}, if there is any influence at all. Therefore, for typical compositions of the COIL active medium, where $K_d \gg \delta K_d$, the contribution of reactions 10, 11 at the stage of initiating the iodine dissociation plays no essential role.

The growth of the I* concentration facilitates the efficiency of reaction chains 2–4, 3→7, 8, 10, 11, and reaction 15. It is known that in the process of recombination $I + I + I_2 \rightarrow 2I_2$, a stable intermediate complex $I-I_2$ is formed with the binding energy about 5 kcal mol^{-1}, which provides a large rate constant of this reaction, equal nearly to 4×10^{-30} cm^6 s^{-1} [32]. Suppose that in process 15, the formation of the intermediate electronically excited complex I^*-I_2 is also possible. The rate of iodine dissociation in the active medium of the COIL due to reaction 15 will be comparable with that due to reactions 1–4 if $k_{15} n_{I^*} n_a \approx n_b k_2$ or $k_2 n_{I_2} + k_5(H_2O) n_{H_2O} \approx (k_2 k_4/k_{15}) \times [1 + n_a/(K n_{I^*})]$. Provided that $k_{15} = 4\times10^{-30}$ cm^3 s^{-1}, this equality is valid for $n_{H_2O} \approx 10^{18}$ cm^3 or $n_{I_2} \approx 7\times10^{16}$ cm^3, which is significantly higher than the concentration of water and iodine in the active medium of the COIL. Therefore, the contribution of reaction 15 to the iodine dissociation can be neglected even assuming that $k_{15} = 4\times10^{-30}$ cm^3 s^{-1}.

In further experiments we used such compositions of the oxygen–iodine medium, for which $\Gamma_b \gg k_2 n_{I_2}$ and $\Gamma_b^{-1} \ll L_{ODS}/V$. Practically it meant that along the ODS the concentration of O_2(b) was close to the quasi-stationary value, determined by formula (1). Then, without taking reactions 6, 14 and 15 into account, the iodine dissociation is described by the equation

$$V\frac{dn_{I_2}}{dz} = -k_2 n_b n_{I_2} - \hat{k}_7 n_{I^*} n_{I_2} - \hat{k}_{11} n_a n_{I_2}, \qquad (6)$$

where $\hat{k}_7 = \hat{k}_{7a} + \hat{k}_{7b}$; and $\hat{k}_{11} = \hat{k}_{11a} + \hat{k}_{11b}$. Form the results of measuring n_b, n_{I^*} and V we calculated the values of

$$Z_b = \frac{1}{V}\int_0^z k_2 n_b(x)\,dx, \quad Z_I = \frac{1}{V}\int_0^z k_7 n_{I^*}(x)\,dx, \qquad (7)$$

where $k_2 = 8.3\times10^{-11}$ cm^3 s^{-1}, and $k_7 = 3.6\times10^{-11}$ cm^3 s^{-1} [33]. Let us introduce the parameter

$$R = \frac{k_7 (n_{I^*})_{max}}{n_b^0 k_2 (1 + K(n_{I^*})_{max}/n_a)},$$

where $(n_{I^*})_{max}$ is the maximal concentration of iodine atoms, achieved in the ODS. Let us call the sum $Z_b + Z_I$ the reduced distance along the ODS. Figure 3 presents the concentration of the iodine atoms versus the reduced distance at different values of R. Figure 3 also shows the plot of the analytic dependence

$$n_I(z)/(2n_{I_2}^0) = 1 - \exp[-(Z_b + Z_I)], \qquad (8)$$

which describes the rate of the atomic iodine production for $\hat{k}_7 = k_7$ and $\hat{k}_{11} = 0$. It is seen that the iodine dissociation is well described by dependence (8) for a wide range of R values. At small R, when $Z_b \gg Z_I$, the iodine dissociation occurs virtually in the reaction sequence 1–4 only. If simultaneously the inequalities $R \ll 1$ and $n_{I^*} > n_a/K$ are valid, then the chain mechanism 2–4 prevails over the initiating mechanism 1–2. Small values of the parameter R are implemented in the media, for which the inequality $k_7 n_a/(n_b^0 k_2 K) \ll 1$ is valid. In the mixture $O_2-I_2-H_2O$, this condition is fulfilled if $n_{H_2O}/n_{O_2} \ll k_1 k_2 K Y/(k_5(H_2O) k_7)$, where $Y = n_a/n_{O_2}$ is the content of singlet oxygen. For example, for $Y = 0.6$ the small values of R are

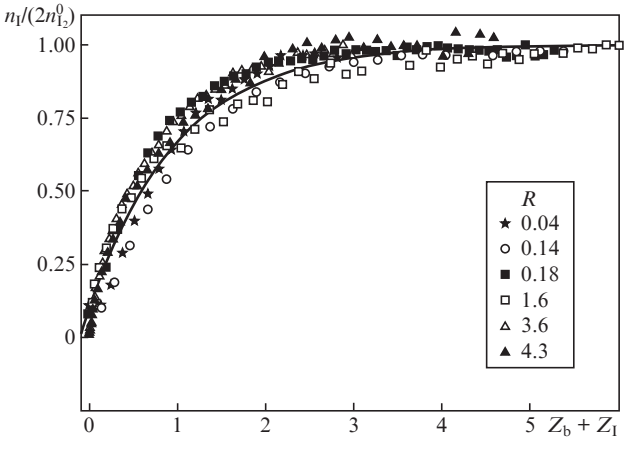

Figure 3. Dependences of the dimensionless concentration of iodine atoms on the parameter $Z_b + Z_I$ at different values of R. The solid curve plots the theoretical dependence (8).

implemented at $n_{H_2O}/n_{O_2} \ll 0.1$. If $R \gg 1$, the dissociation occurs mainly via mechanisms 7, 8.

When $\hat{k}_7 \approx k_7$, the iodine molecules in reaction 7 populate the vibrational reservoir with v in the range 20–40 with the probability $\varphi \approx 1$, and the total rate of reactions 8 essentially exceeds that of the relaxation of iodine molecules from the range 20–40 to the range with $v < 20$. The large value of the constant k_7 can be explained by the formation of the electronically excited complex I_3^* and its subsequent decay into the vibrationally excited molecule I_2 ($20 \leqslant v \leqslant 40$) and the iodine atom in the ground state [34, 35]. Figure 4 shows the variation of the iodine atom concentration as a function of $Z_b + Z_I$ at $R > 1$ and different values of $\Gamma_{I_2 v}$. The dissociation rate is seen to be independent of $\Gamma_{I_2 v}$. According to Ref. [36], $k_9(M) \approx 5\times10^{-12}$ cm^3 s^{-1} for M = Ar, O_2, H_2O, N_2. Substituting the maximal possible value $k_{8b} = 10^{-10}$ cm^3 s^{-1} into the inequality $k_{8a}n_a + k_{8b}n_{I^*} \gg \Gamma_{I_2 v}$ (where $\Gamma_{I_2 v} = 3.5\times10^5$ s^{-1}, $n_a = 10^{16}$ cm^{-3}), we obtain $k_{8a} \gg 3.5\times10^{-11}$ cm^3 s^{-1}. This agrees with the estimate of k_{8a} presented in Ref. [3].

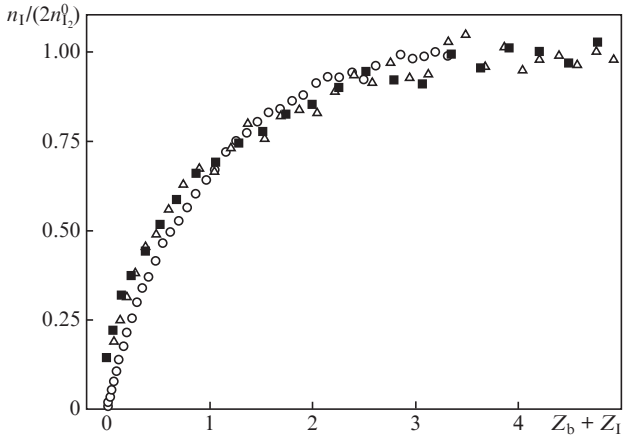

Figure 4. Variation in the concentration of iodine atoms along the gas flow in the ODS at different rates of iodine molecule relaxation form the vibrational energy levels from the range $20 < v < 40$ for $n_a = 1.3\times10^{16}$ cm^{-3}: (○) $\Gamma_{I_2 v} = 1.4\times10^5$ s^{-1}, $R = 1.6$, $(n_{I^*})_{max} = 1.2\times10^{13}$ cm^{-3}; (△) $\Gamma_{I_2 v} = 2.4\times10^5$ s^{-1}, $R = 1.5$, $(n_{I^*})_{max} = 1.4\times10^{13}$ cm^{-3}; and (■) $\Gamma_{I_2 v} = 3.5\times10^5$ s^{-1}, $R = 2.3$, $(n_{I^*})_{max} = 3.2\times10^{13}$ cm^{-3}.

The approximate equality $\hat{k}_{11} \approx 0$ means that the contribution to the iodine dissociation of the reactions involving the vibrationally excited molecules of oxygen is very small, if it exists at all. The reaction involving the atoms I*, which is a source of vibrationally excited oxygen molecules, can be only reaction 4 [4]. The vibrationally excited oxygen molecules can be produced also in reaction 5, but the source of the O_2(b) molecules is also reaction 4. The vibrational energy quanta of the molecules O_2(X), O_2(a), and O_2(b) are very close in value, and due to the fast E–E and V–V exchanges the vibrational energy is distributed over al molecules independent of their electronic state, forming the common reservoir of the vibrational energy [8–10]. The rate of vibrational quanta production in reactions 4 and 5 is $\eta k_4 n_{I^*} n_a$, where η is the total number of vibrational quanta, produced in these reactions. Let us denote by $\Gamma_{O_2 v}$ the rate of vibrational relaxation of the oxygen molecule. Then, the mean number of vibrational quanta in one oxygen molecule above its equilibrium value will be $f = \eta k_4 n_{I^*} Y/\Gamma_{O_2 v}$, the value of n_{I^*} decreasing with decreasing Y. Therefore, the smaller the Y, the smaller the f.

Figure 5 shows the profiles of the concentration n_I, obtained in two experiments with similar initial values of n_a and n_b, but different Y. In these experiments the value of $\Gamma_{O_2 v}$ is mainly determined by the V–T relaxation of the molecules $O_2(v)$ colliding with water molecules, the concentration of which is the same in both cases. The V–T relaxation of $O_2(v = 1)$ occurs in the reactions $O_2(v = 1) + H_2O(v = 0) \leftrightarrow O_2(v = 0) + H_2O(v = 1)$, $H_2O(v = 1) + M \rightarrow H_2O(v = 0) + M$. Under the conditions of the performed experiments, when the relative content of water with respect to oxygen exceeds 10^{-2}, the relaxation of oxygen is determined by the first reaction with the rate constant $k_{O_2-H_2O} \approx 10^{-12}$ cm^3 s^{-1} [37]. The V–T relaxation of O_2(v) at the oxygen molecules and argon atoms occurs with the rate constants $k_{O_2-O_2} = 2.7\times10^{-18}$ cm^3 s^{-1} [37] and $k_{O_2-Ar} < 2\times10^{-16}$ cm^3 s^{-1} [38], that is why in both experiments the value of $\Gamma_{O_2 v}$ is the same. As seen from Fig. 5, the profiles of the concentration n_I are similar in two experiments. This is an evidence in favour of the absence of vibrational nonequilibrium distribution in the oxygen molecules or the miserable contribution of reactions 10, 11 to the dissociation of I_2.

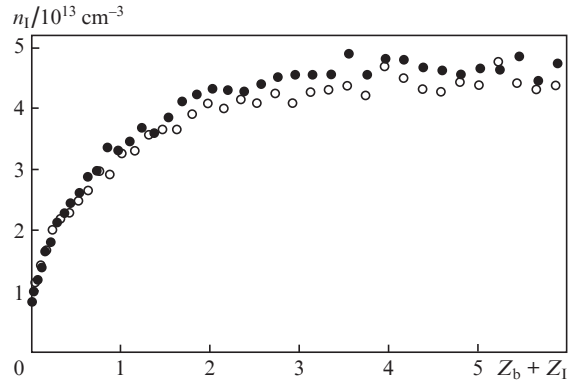

Figure 5. Experimental dependences of n_I on the parameter $Z_b + Z_I$ for the mixture O_2–Ar–H_2O for $n_a(z=0) = 1.3\times10^{16}$ cm^{-3}, $n_b(z=0) = 3\times10^{12}$ cm^{-3}, $\Gamma_b = 25000$: (○) $n_X = 1.4\times10^{16}$ cm^{-3} ($Y = 0.48$), $n_{Ar} = 7.5\times10^{16}$ cm^{-3}; and (●) $n_X = 6\times10^{16}$ cm^{-3} ($Y = 0.18$), $n_{Ar} = 1\times10^{16}$ cm^{-3}.

Figure 6 shows the dependence of the concentration of I*, O_2(a), and O_2(b) on the distance along the ODS using the molecules of H_2O (experiment A) or CO_2 (experiment B). In both experiments the initial concentrations of O_2(b) before mixing the primary flow with that of molecular iodine were the same. It is seen that with the appearance of I* atoms the concentration of O_2(b) grows. Substituting into Eqn (1) the concentrations of particles at the distance of 15 cm from the iodine mixer, the rate constant $k_1 = 4.3\times10^{-17}$ cm^3 s^{-1} and the ratio $K = k_4/k_1 = 6600$, we obtain the quenching probability $\Gamma_b \approx 5\times10^4$ c^{-1}. Thus, in experiment A the water concentration is $n_{H_2O} = \Gamma_b/k_5(H_2O) \approx 10^{16}$ cm^{-3}, and in experiment B the concentration of carbon dioxide is $n_{CO_2} = \Gamma_b/k_5(CO_2) \approx 10^{17}$ cm^{-3}. Assume that f_1 and f_2 exceed their equilibrium values. The V–T relaxation of the oxygen molecules by the CO_2 molecules occurs with the rate constant $k_{O_2-CO_2} = 1.5\times10^{-14}$ cm^3 s^{-1} [9]. Therefore, in experiment A the rate of the V–T relaxation of $O_2(a, v)$ molecules is by 7 times higher than in experiment B. However, as seen from Fig. 6, this fact does not affect the I_2 dissociation rate. In the experiments, the results of which are presented in Figs 5, 6, no excess of vibrationally excited O_2(b) molecules above the equilibrium concentration was detected within the error of the spectral measurements. Thus, we can

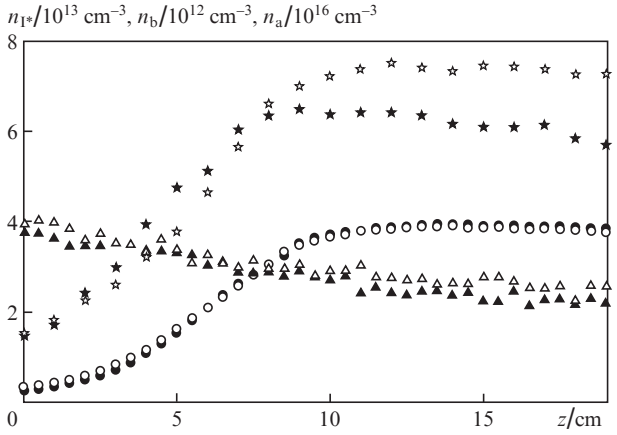

Figure 6. Variation in the concentration of I* (circles), O_2(a) (triangles) and O_2(b) (asterisks) along the gas flow in the ODS with the mixtures O_2–CO_2 (light symbols) and O_2–H_2O (dark symbols).

conclude that at the chain stage of I_2 dissociation the contribution to it from reactions 10, 11 is very small as compared to the contributions of reactions 1–4 and 3→7, 8.

Now let us find the limit concentration of I* atoms, below which the dissociation rate K_d does not depend on it. This situation will take place when in reaction 1 more O_2(b) molecules than in reaction 4 will be produced, and the contribution of reactions 7, 8 to the dissociation rat will be essentially smaller than that of reaction 2. For this purpose during the entire dissociation time the conditions $n_{I*}/n_a \ll K^{-1}$ and $k_2 n_b^0 \gg k_7 n_{I*}$ should be valid. At the minimal concentrations used in the present experiments ($n_a = 10^{16}$ cm^{-3} and $n_b^0 = 5\times10^{11}$ cm^{-3}) both conditions are satisfied if $n_{I*} \ll 10^{12}$ cm^{-3}. As mentioned above, our experiments on the determination of the rate constant for reaction 2 were carried out at $n_{I*} < 10^{11}$ cm^{-3}.

4. Discussion of the results and conclusions

The results of the performed experiments on the iodine dissociation are satisfactorily described by the kinetic scheme proposed in Ref. [3]. Previously, the iodine dissociation rates observed in the experiments both in the active medium of the COIL [13, 14] and in the kinetic experiments [4, 5] could not be explained by the mechanism [3] using the rate constants of reactions 1, 2 and 4, presented in the standard kinetic package (SKP) [39]. In the present paper we found the new values of these constants $k_1 = 4.3\times10^{-17}$ cm^3 s^{-1}, $k_2 = 8.3\times10^{-11}$ cm^3 s^{-1} and $k_4 = 2.8\times10^{-13}$ cm^3 s^{-1} nearly by two times greater than in the SKP. However, the mechanism of reactions 1–4 was still unable to explain the iodine dissociation rate observed in out experiments. Additional reactions 7, 8 taken into account, as proposed in Ref. [3], allow complete explanation of the iodine dissociation rate in our experiments. Similar to Ref. [3], it is necessary to assume that in reaction 7 with the probability close to 1 the iodine molecules are produced in the vibrationally excited states with $v \geqslant 20$, and the dissociation rate of vibrationally excited iodine molecules in reaction 8 considerably exceeds the rate of their loss due to the vibrational relaxation.

Reactions 6, 10 and 14 do not noticeably contribute to the initiation of the iodine dissociation in the active medium of an oxygen–iodine laser. We also did not detect the contribution of reactions 10, 11 to the dissociation at the branching stage. Thus, the hypothesis of the essential role of vibrationally excited molecules O_2(a) in the iodine dissociation is not confirmed by the experiments performed. Since the observed rates of iodine dissociation were not explained based on the kinetic data presented in SKP, the active search for alternative channels of its dissociation was carried out. In Refs [4, 15], the phenomenological mechanism of iodine dissociation was proposed that includes processes 10a and 10b. The rate constants of these processes were considered as the model parameters. Including these processes into the SKP allowed satisfactory description of the dissociation rate in the experiments both with the flow chamber [4, 15] and with the active medium of a supersonic COIL [12–14]. However, to explain the rate of iodine dissociation in our experiments with new increased rate constants for processes 1, 2 and 4, there is no necessity to include processes 10 and 11 into consideration. We have also shown that reaction 15 plays no essential role in the active medium of an oxygen–iodine laser.

The relative contribution of each of the considered mechanisms to the I_2 dissociation depends on the initial composition of the medium. Consider, for example, the kinetics of iodine dissociation in the active medium of an oxygen–iodine laser, the composition of which is close to that used in Ref. [40], namely, $n_{O_2} = 4\times10^{16}$ cm^{-3}, $n_a = 2.4\times10^{16}$ cm^{-3}, $n_{I_2}^0 = 8\times10^{14}$ cm^{-3}, $n_{H_2O} = 2\times10^{15}$ cm^{-3}, $n_b^0 = k_1 n_a^2/(k_5(H_2O)n_{H_2O}) \approx 2.9\times10^{12}$ cm^{-3}. To simplify the analysis let us consider the mixing of the oxygen and iodine-containing flows as instantaneous. Let us take into account the fact that the high energy exchange rate in reaction 3 determines the content of the excited iodine atoms: $n_{I*}/n_I = F_{I*} \approx K_e n_a/[(K_e - 1)n_a + n_{O_2}] \approx 0.8$, where $K_e = 2.85$ is the equilibrium constant of reaction 3 at the temperature 300 K. In the process of dissociation, the concentration of O_2(b) molecules in the first approximation is equal to the quasi-stationary value

$$n_b = \frac{(k_1 n_a + k_4 n_{I*}) n_a}{k_5(H_2O) n_{H_2O} + k_2 n_{I_2}}.$$

In this case the dissociation rate via mechanism 1–4 is

$$D_1 = k_2 n_b n_{I_2} = \frac{k_1 k_2 n_{I_2} n_a^2}{k_5(H_2O) n_{H_2O} + k_2 n_{I_2}} \left(1 + K\frac{n_{I*}}{n_a}\right),$$

and via mechanism 7, 8 it is $D_2 = k_7 n_{I*} n_{I_2}$. The ratio of I_2 dissociation rates via the first and the second mechanism is

$$\frac{D_1}{D_2} = \frac{k_1 k_2 n_a^2}{k_7 F_{I*} n_I (k_5(H_2O) n_{H_2O} + k_2 n_{I_2})} \left(1 + K\frac{F_{I*} n_I}{n_a}\right)$$

$$= \frac{N_1 N_2}{(N_2 - n_I) n_I} \left(1 + \frac{n_I}{N_3}\right),$$

where

$$N_1 = \frac{k_1 k_2 n_a^2}{k_7 (k_5(H_2O) n_{H_2O} + k_2 n_{I_2}) F_{I*}} \approx 10^{12} \text{ cm}^{-3};$$

$$N_2 = \frac{2(k_5(H_2O) n_{H_2O} + k_2 n_{I_2}^0)}{k_2} \approx 1.8\times10^{15} \text{ cm}^{-3};$$

$$N_3 = \frac{n_a}{K F_{I*}} \approx 4.5\times10^{12} \text{ cm}^{-3}.$$

Until in the medium $n_I < 1.3\times10^{12}$ cm^{-3}, the relations $D_1/D_2 > 1$ and $F_{I*}n_I/n_a < K$ will be valid and the dissociation will occur mainly via the initiating mechanism 1, 2. When the concentration of the iodine atoms will grow and the condition $1.3\times10^{12} < n_I < 1.4\times10^{15}$ cm^{-3} will hold, the ratio D_1/D_2 will become smaller than one, and the main contribution to the dissociation will be provided by the mechanism of reactions 7, 8. On the achievement of a large degree of dissociation, when $n_I > 1.4\times10^{15}$ cm^{-3} the inequality $D_1/D_2 > 1$ will become valid again, but the main contribution to the dissociation will be given by the chain mechanism 2–4.

Acknowledgements. The authors are grateful to V.N. Azyazov for fruitful discussions and remarks.

The work at the Samara Branch of the P.N. Lebedev Physics Institute of the Russian Academy of Science was supported within the State Research Task (Project No. 114091840046) and at the Samara State National Research University by the Ministry of Education and Science of the Russian Federation within the framework of the State Research Task to Higher Education Institutions and Research Organisations in the Field of Scientific Activity (Project No. 3.161.2014/K).

References

1. Arnold S.J., Ogryzlo E.A., Witzke H. *J. Chem. Phys.*, **40**, 1769 (1964).
2. Derwent R.G., Kearns D.R., Thrush B.A. *Chem. Phys. Lett*., **6**, 115 (1970).
3. Heidner R.F., Gardner C.E., Segal G.I., El-Sayed T.M. *J. Phys. Chem.*, **87**, 2348 (1983).
4. Azyazov V.N., Pichugin S.Yu., Heaven M.C. *J. Chem. Phys*., **130**, 104306 (2009).
5. Lilenfeld H.V. *Oxygen-Iodine Laser Kinetics* (St. Louis, MO: McDonnell Douglas Research Lab., Final Report, AFWL-TR-83-1, May 1983).
6. Schurath U. *J. Photochem.*, **4**, 215 (1975).
7. Azyazov V.N. *Kvantovaya Elektron*., **39**, 989 (2009) [*Quantum Electron*., **39**, 989 (2009)].
8. Kalogerakis K.S., Copeland R.A., Slanger T.G. *J. Chem. Phys*., **123**, 044309 (2005).
9. Pejaković D.A., Campbell Z., Kalogerakis K.S., Copeland R.A., Slanger T.G. *J. Chem. Phys.*, **135**, 094309 (2011).
10. Bloemink H.I., Copeland R.A., Slanger T.G. *J. Chem. Phys*., **109**, 4237 (1998).
11. Hays G.N., Fisk G.A. *Appl. Phys. Lett*., **42**, 3 (1983).
12. Madden T.J., Noren C.A., Ortiz T., Wilkinson M., Klennert W., Chan R.W., Behrens H.W., Decker R., Walter R. *AIAA Paper*, 2010-1156 (2010).
13. Waichman K., Barmashenko B.D., Rosenwaks S. *J. Chem. Phys.*, **133**, 084301 (2010).
14. Waichman K., Barmashenko B.D., Rosenwaks S. *J. Chem. Phys.*, **136**, 244307 (2012).
15. Azyazov V.N., Heaven M.C. *AIAA J.*, **44**, 1593 (2006).
16. Zagidullin M.V., Malyshev M.S., Azyazov V.N. *Kvantovaya Elektron*., **45**, 720 (2015) [*Quantum Electron*., **45**, 720 (2015)].
17. Zyryanov S.M., Lopayev D.V. *Fiz. Plazmy*, **33**, 1 (2007) [*Plasma Phys. Rep*., **33**, 510 (2007)].
18. Zagidullin M.V., Khvatov N.A., Nyagashkin A.Yu. *Kvantovaya Elektron*., **41**, 135 (2011) [*Quantum Electron*., **41**, 135 (2011)].
19. Zagidullin M.V., Khvatov N.A., Malyshev M.S., Svistun M.I. *J. Phys.Chem A.*, **116**, 10050 (2012).
20. Zagidullin M.V., Khvatov N.A., Malyshev M.S. *Khim. Fiz*., **30**, 3 (2011) [*Russ. J. Phys. Chem. B*, **5** (6), 969 (2011)].
21. Heidner R.F., Gardner C.E., El-Sayed T.M., Segal G.I., Kasper J.V.V. *J. Chem. Phys*., **74**, 5618 (1981).
22. Noxon J.F. *J. Chem. Phys*., **52**, 1852 (1970).
23. Azyazov V.N., Mikheyev P., Postell D., Heaven M.C. *Chem. Phys. Lett*., **482**, 56 (2009).
24. Atkinson R., Baulch D.L., Cox R.A., Crowley J.N., Hampson R.F., Hynes R.G., Jenkin M.E., Rossi M.J., Troe J. *Atmos. Chem. Phys*., **4**, 1461 (2004).
25. Lilenfeld H.V., Carr P.A.G., Hovis F.E. *J. Chem. Phys*., **81**, 5730 (1984).
26. Derwent R.G., Thrush B.A. *Trans. Faraday Soc.*, **67**, 2036 (1971).
27. Heidner R.F. *J. Photochem.*, **25**, 449 (1984).
28. Han J.D., Komissarov A.V., Tinney S.P., Heaven M.C. *Proc. SPIE Int. Soc. Opt. Eng.*, **5777**, 198 (2005).
29. Muller D.F., Young R.H., Houston P.L., Wiesenfeld J.R. *Appl. Phys. Lett*., **38**, 404 (1981).
30. Howard C.J. *J. Phys. Chem*., **83**, 3 (1976).
31. Zagidullin M.V. *Kvantovaya Elektron*., **40**, 794 (2010) [*Quantum Electron.*, **40**, 794 (2010)].
32. Blake J.A., Burnes G. *J. Chem. Phys.*, **54**, 1480 (1971).
33. Burde D.H., McFarlane R.A. *J. Chem. Phys.*, **64**, 1850 (1976).
34. Hofmann H., Leone S.R. *J. Chem. Phys.*, **69**, 641 (1978).
35. Hall G.E., Marinelli W.J., Houston P.L. *J. Phys. Chem*., **87**, 2153 (1983).
36. Lawrence W.G., Van Marter T.A., Nowlin M.L., Heaven M.C. *J. Chem. Phys*., **106**, 127 (1997).
37. Huestis D.L. *J. Phys. Chem*., **110**, 6638 (2006).
38. Collins R.J., Husain D. *J. Photochem*., **1**, 481 (1972).
39. Perram G.P. *Int. J. Chem. Kinet*., **27**, 817 (1995).
40. Zagidullin M.V., Nikolaev V.D., Svistun M.I., Khvatov N.A. *Kvantovaya Elektron*., **35**, 907 (2005) [*Quantum Electron*., **35**, 907 (2005)].